Korean J. Chem. Eng., 36(9), 1455-1465 (2019)
DOI: 10.1007/s11814-019-0347-2

pISSN: 0256-1115
eISSN: 1975-7220

Polyethylenimine-crosslinked chitin flake as a biosorbent for removal of Acid Blue 25

Gyeong Min Kim*, Zhuo Wang, Su Bin Kang**, and Sung Wook Won*,**,†**

*Department of Marine Environmental Engineering, Gyeongsang National University,
2 Tongyeonghaean-ro, Tongyeong, Gyeongnam 53064, Korea
**Department of Ocean System Engineering, Gyeongsang National University,
2 Tongyeonghaean-ro, Tongyeong, Gyeongnam 53064, Korea
(*Received 3 April 2019 • accepted 23 July 2019*)

Abstract−A chitin-based biosorbent that can be used to effectively remove dyes, typical color inducers in industrial wastewater, was developed. The crosslinking agent glutaraldehyde was bonded to the hydroxyl and/or amine groups of chitin, and then polyethylenimine (PEI), a cationic polymer, was cross-linked to produce PEI-chitin. The successful preparation of PEI-chitin was confirmed using FE-SEM, BET and FTIR analysis and simple adsorption evaluation. The adsorption performance of PEI-chitin was assessed by Acid Blue 25, in terms of the pH effect, isotherm adsorption, adsorption kinetic and thermodynamic parameters. Based on the Langmuir model the maximum dye uptake at pH 2 was 177.32 mg/g, and the adsorption equilibrium was attained within 120 and 500 min for two different dye concentrations (50 and 100 mg/L). Desorption experiments were evaluated using 0.001-1 M NaOH, $NaHCO_3$, and Na_2CO_3 as eluents. The desorption rate was highest (85.2%) when 0.01 M NaOH was employed as the eluent. It was found that the developed biosorbent could be repeatedly used three times through adsorption-desorption of Acid Blue 25.

Keywords: Chitin, Biosorbent, Acid Dye, Surface Modification, Polyethylenimine

INTRODUCTION

For decades, dyes have often been utilized in the textile, paper, pharmaceutical, plastic, leather, cosmetic, rubber, and food industries [1]. More than 100,000 commercial dyes and pigments are available, and more than 7×10^5 tons per year are produced worldwide [2]. In the fiber dyeing process, a significant amount of wastewater is generated, in which dyes account for approximately 10-15%. Notably, the dyes are also discharged along with the wastewater [3]. In general, 1,000 mg/L of dye is used as a staining solution, and 100 mg/L of dye remains in the staining wastewater [4]. As such, the discharge of dark-colored wastewater can reduce the photosynthesis of aquatic organisms by suppressing the penetration of sunlight. In addition, some dyes have been reported to produce toxic, carcinogenic, and mutagenic intermediates via hydrolysis and oxidation, posing a threat to both nature and humans [5,6]. However, it is difficult to decompose or remove most dyes using conventional wastewater treatment processes, as they are non-biodegradable synthetic materials containing chemically complex aromatic molecular structures [7]. Dyed wastewater can be treated using methods such as coagulation/solidification, chemical oxidation, adsorption, membrane separation, biological treatment, ozone treatment, photocatalysis, filtration, electrochemistry, and membrane treatment [8,9]. Among them, the adsorption process can be regarded as one of the ideal techniques for dye treatment due to its high efficiency, good capacity, applicability and high regeneration efficiency, and recycling potential of the adsorbents [2,6,10]. Therefore, before discharging dye-bearing wastewaters into the environment, removing the dyes using an eco-friendly adsorption technology is of importance.

Chitin is the world's second most abundant polysaccharide material and is a low-cost, biodegradable, and regenerable biopolymer with dense structures containing hydroxyl and *N*-acetyl groups. These natural polymers can be extracted from fungi, insect exoskeleton, and shells of crustaceans, such as crayfish, shrimp, and crabs, and are also found in invertebrates such as sponges [11]. In addition, chitin can be obtained from seafood industrial wastes, the recycling of which contributes to environmental protection and waste management. Despite the advantages of chitin, there have been few studies on the application of chitin to dye removal due to its small surface area, and high crystallinity [12]. Chitosan, an amino-rich biosorbent, which is derived from deacetylation of chitin, has been extensively studied for dye containing wastewater treatment. However, chitosan has low mechanical strength, high solubility, and easy hydrolysis under acidic conditions, which has limited its application in dye wastewater treatment. On the other hand, it has highly crystallinity, which not only enables its good physical stability but also excellent chemical stability in various acidic, basic, and organic solvents [13]. Moreover, it has *N*-acetyl groups and a hydroxyl groups on its surface which makes its surface able to be modified to improve the adsorption performance of chitin [14]. Chemical crosslinking is one of the most effective ways to improve the adsorption performance of adsorbents. However, such modifications can cause loss of amine groups and hydroxyl groups, resulting in a decrease in adsorption performance [15]. To prevent this disadvantage, polymeric materials that contain a significant number of amine groups are required, and typically used reagent was polyethylenimine (PEI), which is alkaline water-soluble functional macro molec-

†To whom correspondence should be addressed.
E-mail: sungukw@gmail.com

ular. PEI contains a large amount of N-donor atoms with primary, secondary and ternary amino groups in a ratio of approximately 1 : 2 : 1 [16,17]. Through the cross-linking agent GA, the cross-linking between the amine group of PEI and the functional groups of the chitin surface is formed, thereby enhancing its adsorption performance by imparting a large amount of amine groups [15]. Therefore, chitin, which is difficult to use as an adsorbent, has excellent adsorption performance. In addition, by using raw chitin without deacetylation process, it is possible to prevent the production of large quantities of wastewater by deacetylation.

In the present work, a simple surface modification method for cross-linking PEI on the surface of chitin was developed to produce a chitin-based adsorbent for the removal of anionic dyes. Thus, a PEI cross-linked chitin adsorbent (PEI-chitin) was developed. To confirm the successful preparation of the adsorbent, field emission scanning electron microscopy (FE-SEM), specific surface area analysis using Brunauer-Emmett-Teller (BET) method and Fourier transform infrared (FTIR) analysis were carried out, and a simple adsorption evaluation was performed on an acid dye, i.e., Acid Blue 25 (AB25). In addition, the overall adsorption/desorption performance of PEI-chitin was assessed in terms of the pH effect, isotherm adsorption, adsorption kinetic and thermodynamic parameters, desorption efficiency, and reusability.

EXPERIMENT

1. Experimental Materials

The practical grade of chitin was supplied by Young Puk Chemical Co., Ltd., and chitin having a size in the range of 180-300 μm was used in all experiments. PEI with 70,000 M.W. and 50% purity was obtained from Habjung Moolsan Co., Ltd. and glutaraldehyde (GA) with 25% purity were obtained from Junsei Chemical Co., Ltd., respectively. Model acid dye, AB25 was obtained from Sigma-Aldrich Korea. Table 1 lists the general characteristics of AB25. The other chemicals with analytical grade were used without further pretreatment.

2. Preparation of PEI-chitin

A mixture consisting of chitin flake (5 g) and 3% GA solution (100 mL) was mixed in a shaking incubator at 25 °C and 160 rpm for 2 h. GA-chitin was washed with 400 mL of distilled water to get rid of unreacted GA from the chitin surface and then it was immediately transferred to 100 mL of 10% PEI solution and reacted at 25 °C and 160 rpm for 30 min. As a result, PEI-chitin was obtained. Fig. 1 shows the overall reaction process involved in the preparation of PEI-chitin. The PEI-chitin separated using the solid-liquid separation method was washed three times with distilled water. Thereafter, PEI-chitin was lyophilized at −100 °C for 24 h.

3. FE-SEM, BET and FTIR Analyses

The samples prepared to examine the surface changes in chitin after surface area modification were observed at magnification factors of 500 and 5,000 using FE-SEM (JSM-7610F, Jeol, Japan). The specific surface and pore size distribution of biosorbent was determined via N_2 adsorption-desorption isotherm using a specific surface area analyzer (3 Flex, Micromeritics, USA). An FTIR spectrometer (VERTEX 80v, BRUKER, USA) was used to observe any changes in the functional groups following the surface modification, and the spectrum was examined in the range of 4,000-400 cm^{-1}. The samples were evenly ground with KBr powder and compressed to obtain pellets for analysis.

4. Batch Adsorption Experiments

Batch adsorption experiments were performed to evaluate the effects of variables such as pH, dye concentration, time, and temperature, which are known to be important parameters in the adsorption process. The experiments were performed using a 50 mL polypropylene conical tube containing 30 mL of dye and 0.02 g of PEI-chitin placed in a multi-shaking incubator at 160 rpm and 25 °C. The pH effect experiment was investigated for the relationship between the final pH and the dye uptake, to analyze the adsorption of AB25 by PEI-chitin. Each tube was adjusted differently for pH ranging from 2 to 12 using 0.1, 1, and 5 M HCI and NaOH and stirred sufficiently at 160 rpm at 25 °C for 24 h. During the adsorption experiment, the pH in each tube was kept constant, and the final pH was measured after attaining adsorption equilibrium. Adsorption kinetic experiments were evaluated at initial dye concentrations of 50 and 100 mg/L to determine the time required to attain adsorption equilibrium at pH 2. The residual dye concentration of each sample taken at a particular time was analyzed using a UV-Vis spectrophotometer (X-MA3000PC, Human Co., Ltd., Korea). Isotherm experiments were examined at four different temperatures to evaluate the maximum adsorption amount of AB25 by PEI-chitin. The experiments were conducted at a pH of 2 for 24 h with initial dye concentrations varying from 0 to 300 mg/L. Analytical samples were prepared to analyze the dye concentration remaining in each sample.

The analytical samples were prepared by centrifugation at 9,000 rpm for 5 min, followed by collecting only the supernatant and appropriately diluting with distilled water. The absorbance was measured by UV-Vis spectrophotometer at 600 nm, which is the maximum wavelength of AB25. The dye uptake q (mg/g) can be calcu-

Table 1. General characteristics of Acid Blue 25

Structure	*M.F.	** M.W.	Dye content (%)	λ_{max} (nm)
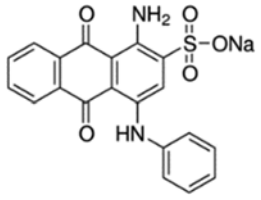	$C_{20}H_{13}N_2NaO_5S$	416.38	45	600

*M.F: molecular formula, **M.W: molecular weight

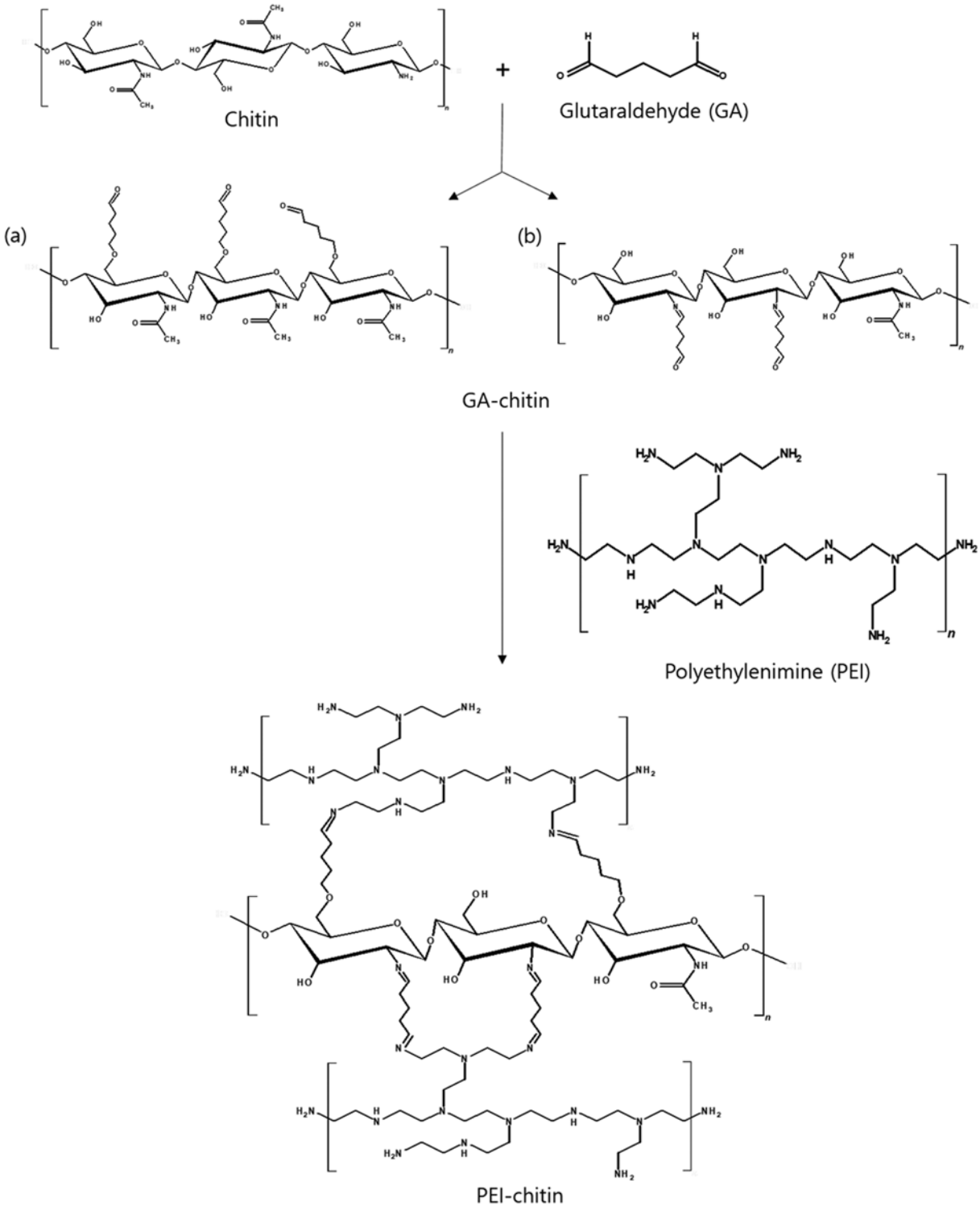

Fig. 1. Schematic of reaction pathway for fabrication of PEI-chitin: (a) crosslinked with hydroxyl group; (b) crosslinked with amine group.

lated using Eq. (1).

$$q = \frac{C_i V_i - C_f V_f}{m} \quad (1)$$

In this equation, C_i and C_f (mg/L) denote the initial and final AB25 concentrations, respectively, and V_i and V_f (L) denote the initial and final solution volumes, respectively; m (g) represents the amount of PEI-chitin based on dry weight.

5. Adsorption Data Modeling

The isotherm experiments data were estimated by the Langmuir, Freundlich, and Redlich-Peterson models, respectively. These models can be expressed as follows.

$$\text{Langmuir model: } q_e = \frac{q_{max} b_L C_e}{1 + b_L C_e} \quad (2)$$

$$\text{Freundlich model: } q_e = K_F C_e^{1/n} \quad (3)$$

$$\text{Redlich-Peterson model: } q_e = \frac{K_{RP} C_e}{1 + a_{RP} C_e^{\beta}} \quad (4)$$

where q_e (mg/g) is the dye uptake, and C_e (mg/L) the concentration of AB25 present in the solution at equilibrium. q_{max} (mg/g) is the maximum dye uptake, and b_L (L/mg) the Langmuir constant, which represents the affinity between the adsorbent and the adsorbate. K_F (L/g) and n are Freundlich constants, which means the adsorption capacity and adsorption strength of the adsorbent, respectively. K_{RP} (L/g) and a_{RP} (L/mg)$^{\beta}$ are Redlich-Peterson constant. β is the Redlich-Peterson exponent which lies between 0 and 1. This model has two limiting cases, which can be explained as follows:

When β=1, the Langmuir equation results, given by

$$q_e = \frac{AC_e}{1 + BC_e} \quad (5)$$

When β=0, Redlich-Peterson equation transforms to Henry's law equation results;

$$q_e = \frac{AC_e}{1 + B} \quad (6)$$

To clarify information on energy change related to adsorption and feasibility and process characteristics (exo- or endothermic, and physi- or chemisorption), thermodynamics were evaluated. The main thermodynamic parameters include the Gibbs free energy change (ΔG), enthalpy change (ΔH), and entropy change (ΔS). ΔG can be calculated using Eq. (7), where b_L is the Langmuir constant at temperature T, R is the ideal gas constant (8.314 J/mol K), and T is the temperature of the aqueous solution (K). The relationship between ΔG, ΔH, and ΔS is expressed in Eq. (8).

$$\Delta G = -RT \ln b_L \quad (7)$$

$$\Delta G = \Delta H - T\Delta S \quad (8)$$

Using Eqs. (7) and (8), the following van't Hoff equation was obtained, and the ΔH and ΔS values can be calculated accordingly.

$$\ln b_L = -\frac{\Delta H}{RT} + \frac{\Delta S}{R} \quad (9)$$

The ΔH and ΔS values can be calculated using the y-intercept and slope values in the $\ln b_L$ vs 1/T graph. Table 4 lists the thermodynamic parameters calculated using Eqs. (7) and (9).

To understand the adsorption kinetics of the rate constants, the experimental data are described using pseudo-first-order and pseudo-second-order kinetic models, which are expressed in the following non-linear equations.

Pseudo-first-order kinetic model:

$$q_t = q_1(1 - \exp(-k_1 t)) \quad (10)$$

Pseudo-second-order kinetic model:

$$q_t = \frac{q_2^2 k_2 t}{1 + q_2 k_2 t} \quad (11)$$

Here, q_t (mg/g) represents the adsorption amount at time t, and q_1 and q_2 (mg/g) represent the adsorption amount at the equilibrium state; and k_1 (L/min) and k_2 (g/mg min) denote the pseudo-first-order and pseudo-second-order rate constants, respectively. The initial adsorption rate h (mg/g min) as $t \rightarrow 0$ is defined as shown in Eq. (12).

$$h = k_2 q_2^2 \quad (12)$$

6. Desorption and Reuse Experiment

The dye-sorbed PEI-chitin was prepared by adding 0.02 g of PEI-chitin to 30 mL of aqueous dye solution (100 mg/L) and subsequently stirring at a pH of 2 for 24 h. Three different chemicals, NaOH, $NaHCO_3$, Na_2CO_3, were selected as the eluents to determine the effective desorption conditions related to the adsorbed AB25. The concentration of the eluent was varied from 0.001 to 1 M in the desorption experiments. The desorption efficiency can be calculated using Eq. (13).

$$\text{Desorption efficiency (\%)} = \frac{\text{Amount of desorbed dye (mg)}}{\text{Amount of initially adsorbed dye (mg)}} \times 100 \quad (13)$$

The reusability of the adsorbent was evaluated by repeatedly performing the adsorption and desorption experiments three times. The adsorption experiments were carried out at pH 2, while the desorption experiments were examined using 0.01 M NaOH as the eluent.

RESULTS AND DISCUSSION

1. Verification of Surface Modified Chitin

To investigate the main characteristic changes on the surface of chitin following surface modification, FE-SEM analyses were performed on raw chitin, GA-chitin, and PEI-chitin. Fig. 2 shows the results. As shown in Fig. 2(a), the surface of chitin, which is observed at a magnification factor of 500, seems to be smooth and flat. However, in the image magnified by 5,000 times (Fig. 2(a′)), the surface is found to be rough and heterogeneous with somewhat fine pores. On the other hand, the surface of chitin after GA treatment is found to be rough and wrinkled when observed at a magnification factor of 500 compared to raw chitin (Fig. 2(b)), whereas the 5,000-fold magnified image (Fig. 2(b′)) shows that the surface is relatively smooth with increased pore size. In the case of PEI-chitin with the GA-chitin surface cross-linked with PEI, PEI is well distributed throughout the chitin surface, as shown in Fig. 2(c). The image taken at a magnification factor of 5,000 (Fig. 2(c′)) shows the above results more clearly, and larger and greater number of pores are present on the chitin surface.

The specific surface area of the adsorbent was analyzed through adsorption-desorption of N_2 (Fig. 3). Adsorption isotherms showed three distinct areas. First, a gentle rising curve due to the initial adsorption of nitrogen was observed at P/Po<0.05, next, stagnation was observed between 0.05<P/Po<0.8. Finally, at 0.8<P/Po, the curve was raised sharply to reach equilibrium. This isotherm showed a type II morphology, and the shape of the isotherm was present at a high rate of micropores and showed some meso- and macropores. The average adsorption volume of raw chitin was 2.9×10^{-2}

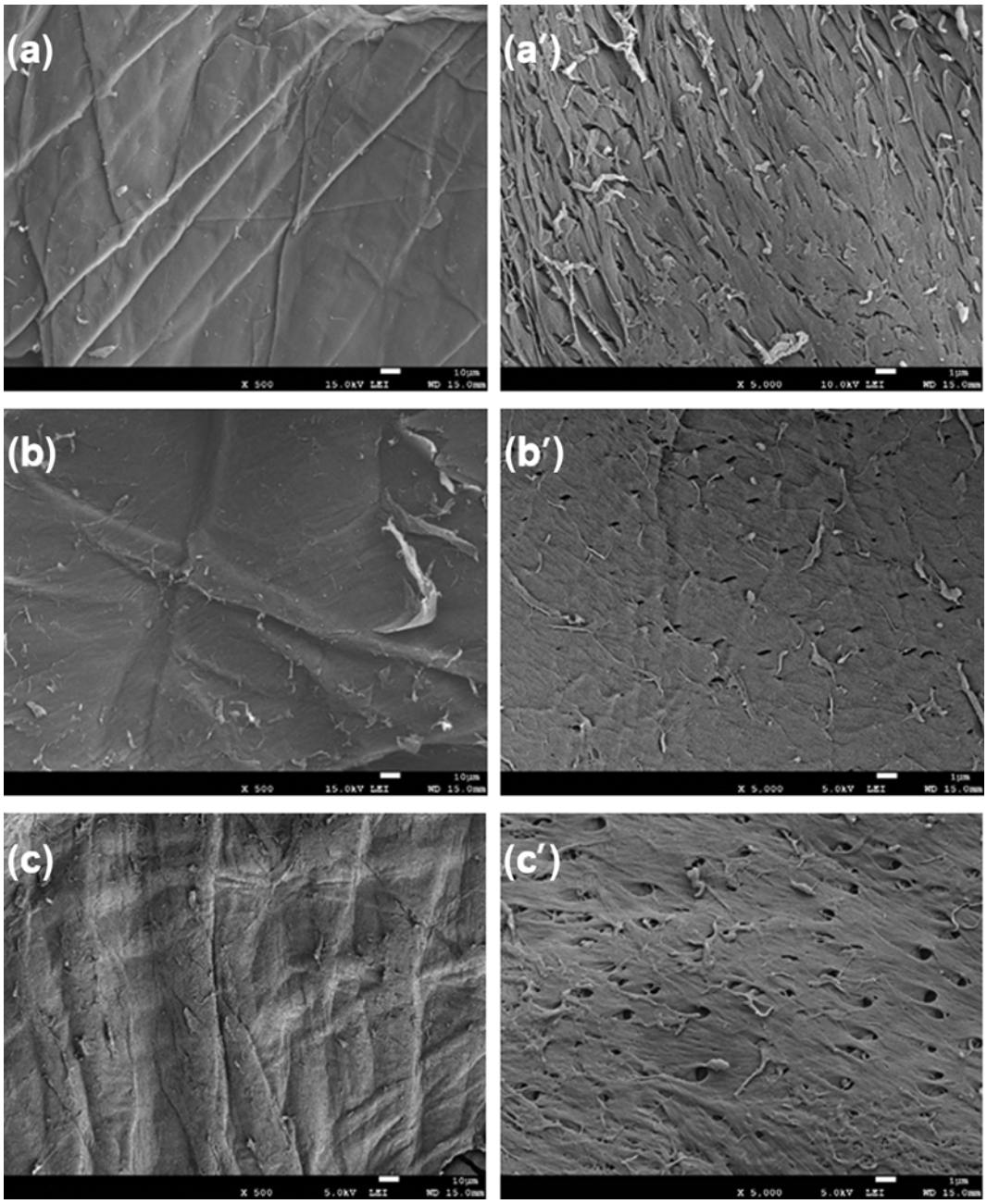

Fig. 2. FE-SEM images of raw chitin ((a) and (a′)), GA-chitin ((b) and (b′)), and PEI-chitin ((c) and (c′)): ((a), (b), and (c)) magnification of ×500; and ((a′), (b′), and (c′)) magnification of ×5,000.

cm^3/g, while that of GA-chitin was 1.8×10^{-2} cm^3/g, and PEI-chitin, the average adsorption volume tended to decrease as the surface modification step progressed to 1.4×10^{-2} cm^3/g. However, the mean pore diameter was measured to be 47.11 nm, which was about 1.18-fold higher for PEI-chitin compared to 39.82 nm for raw chitin. This is similar to the result of SEM image. The BET surface area decreased by about 0.49-times from 4.24 m^2/g for raw chitin and 2.09 m^2/g for PEI-chitin. The decrease in the volume and BET surface area of the pores can be expected to be due to the chemical adsorption rather than the physical adsorption by pore-chitin adsorption.

An FTIR analysis was performed to determine the difference between the samples in terms of the formation of functional groups at each stage in the PEI-chitin preparation process (Fig. 4). The spectra for raw chitin, GA-chitin, and PEI-chitin show a similar pattern overall. Nevertheless, a characteristic peak change is observed following surface modification. Won et al. [17] reported a similar result that the peak in the range of 3,600-3,200 cm^{-1} indicates N-H and O-H stretching vibration in the amine and hydroxyl groups. The peak near 2,923 cm^{-1} indicates the deformation vibration of the methyl group ($-CH_3$) and C-H symmetric stretching of the methylene group ($-CH_2$). The peak at 1,635 cm^{-1} represents a C=N bond, showing a slight increase for GA-chitin compared to that for raw chitin, and the strongest peak is observed for PEI-chitin. This change

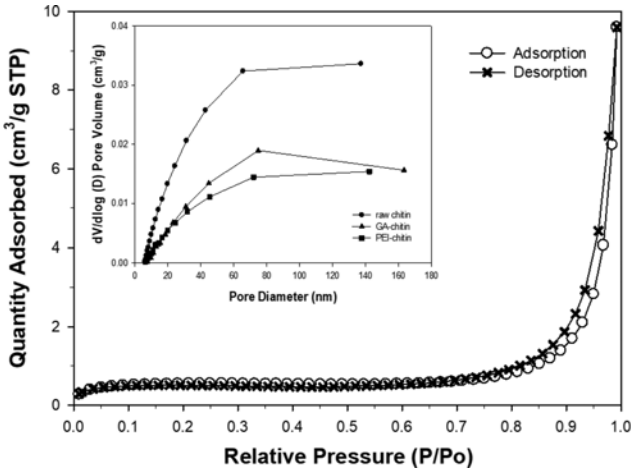

Fig. 3. Nitrogen adsorption-desorption isotherm of PEI-chitin and Barrett-Joyner-Halenda (BJH) pore size distribution plots (inset) of raw chitin, GA-chitin and PEI-chitin.

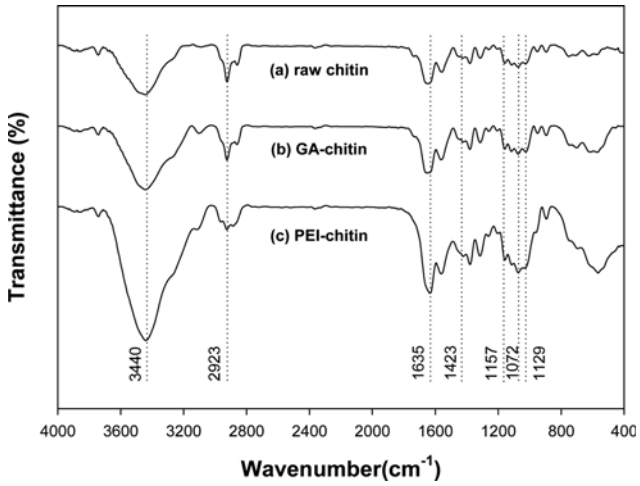

Fig. 4. FTIR spectra of (a) raw chitin, (b) GA cross-linked chitin (GA-chitin), and (c) PEI-crosslinked chitin (PEI-chitin).

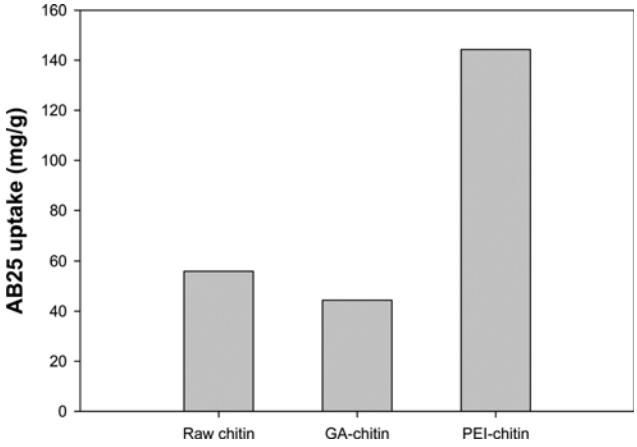

Fig. 5. Comparison of AB25 adsorption by raw chitin, GA-chitin, and PEI-chitin ($C_{i\ AB25}$: 100 mg/L, PEI-chitin dosage: 0.02 g, pH: 2.0, reaction time: 24 h at 25 °C).

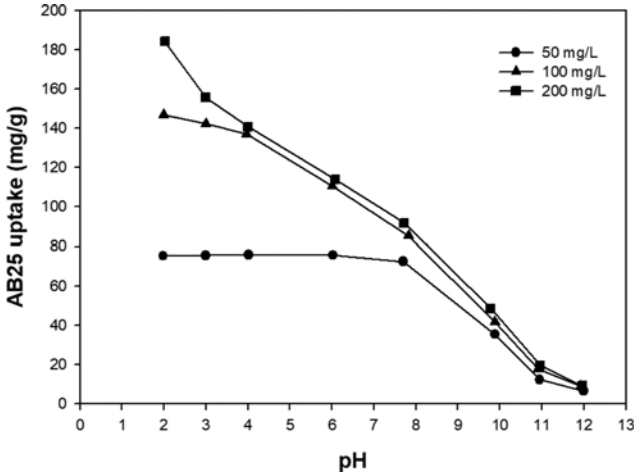

Fig. 6. Effect of pH on AB25 adsorption by PEI-chitin ($C_{i\ AB25}$: 50, 100, and 200 mg/L, PEI-chitin dosage: 0.02 g, pH: 2.0-12.0, reaction time: 24 h at 25 °C).

indicates that the bonding between the amine group of chitin or PEI and the carboxyl group of GA is either by Schiff base reaction or by Michael addition reaction, showing that PEI is effectively bound to the chitin surface [18]. The peaks at 1,157, 1,072, and 1,129 cm^{-1} correspond to C-O-C stretching and C=O stretching, indicating that the hydroxyl groups in the chitin molecule are involved in the bonding with GA [18,19]. Choi et al. [20] reported that the main characteristic peaks of PEI are 1,423 cm^{-1} (-NH bending and deformation vibration), 1,650 cm^{-1} (-NH_2 or -NH), and 3,440 cm^{-1} (N-H stretching). At these peaks, raw chitin and GA-chitin show a similar peak change; however, the peak intensity of PEI-chitin increases significantly. Therefore, the above peak changes suggest the successful introduction of PEI on the chitin surface.

Fig. 5 displays the comparison results of samples in terms of the amount of adsorption to 100 mg/L of AB25 at each step. The uptakes of raw chitin, GA-chitin, and PEI-chitin are 55.93, 44.35, and 144.28 mg/g, respectively; the uptake of GA-chitin is approximately 20.7% lower than that of raw chitin. This phenomenon may have resulted from a decrease in the number of functional groups involved in the dye adsorption process, because of the binding of some of the amine groups present in chitin to GA. On the other hand, the adsorption amount of PEI-chitin increased by approximately 2.6-times compared to that of raw chitin. This may have resulted from the increase in the number of amine groups owing to the cross-linking of PEI onto the chitin surface. Thus, this study experimentally confirms the successful cross-linking of PEI on the surface of chitin.

2. Effect of pH

pH is one of the most significant valuables affecting the total adsorption process and adsorption amount because of its chemical influence on the adsorbent surface during the dye adsorption process. To investigate the effect of pH on the adsorption of AB25 by PEI-chitin, an experiment was performed at three different dye concentrations (50, 100, and 200 mg/L) from pH 2.0 to 12.0 (Fig. 6). The amount of adsorption to AB25 tends to decrease with the increase in the pH, and the optimum pH for the adsorption of

AB25 by PEI-chitin is 2.0. For a dye concentration of 50 mg/L, a similar adsorption amount is observed in the pH range of 2-8, and the removal rate of AB25 is 99% in the pH range of 2-6 and 95% or more at a pH of 8. The results confirm that PEI-chitin shows a high removal rate of 95% or more in a wider pH range when the dye concentration is low. On the other hand, the adsorption amounts for 100 and 200 mg/L are significantly different in terms of the pH, probably because the number of dye molecules was more than the number of adsorbent binding sites, leading to competitive adsorption. In particular, hydrogen ions act as bridges between the adsorbent and the dye molecules, and the number of hydrogen ions decreases with the increase in the pH. This, in turn, could have reduced the ionic interactions between the adsorbent and the adsorbate, thereby decreasing the adsorption amount.

Examining the states of the adsorbent and adsorbate present in the aqueous solution helps explain the mechanism of adsorbate adsorption to the adsorbent. AB25 rapidly dissolves in this solution, and the sulfonate (D-SO_3Na) of the dye disassociates and converts to anionic dye ions, as follows.

$$\text{D-SO}_3\text{Na}(l) \xrightarrow{H_2O} \text{D-SO}_3^-(l) + \text{Na}^+(\text{aq}) \quad (14)$$

On the other hand, the amine group of PEI-chitin is protonated in the presence of H^+, being charged positively.

$$\text{PEI-chitin-NH}_2(\text{s}) + \text{H}^+(\text{aq}) \rightleftarrows \text{PEI-chitin-NH}_3^+(\text{s}) \quad (15)$$

These counterions easily bond because of the interactions between the ions.

$$\text{PEI-chitin-NH}_3^+(\text{s}) + \text{D-SO}_3^-(l) \rightleftarrows \text{PEI-chitin-NH}_3^+(\text{s})\ldots_3^-\text{OS-D}(l) \quad (16)$$

Thus, the main adsorption mechanism between PEI-chitin and AB25 can be explained by the electrostatic attraction between the protonated amine groups of PEI-chitin and the anionic sulfonic parts of AB25. In fact, Wong et al. [21] revealed that acidic dyes, such as Acid Green 25, Acid Orange 10, Acid Orange 12, Acid Red 18, and Acid Red 73, were bound to the amine groups in chitosan by electrostatic attractive forces, and that the difference in the degree of adsorption could be attributed to the chemical structure of each dye. Sun et al. [22] reported similar results on the adsorption of Acid Red 18 by a PEI-grafted anaerobic granular sludge.

3. Isothermal Adsorption Curve and Modeling

Understanding the appropriate correlation to the equilibrium curve is important and meaningful in optimizing the design of the adsorption system for dye removal in aqueous solution. In addition, an isotherm experiment is frequently used to confirm the adsorption equilibrium relationship between the adsorbent and the adsorbate; also, the theoretical maximum sorption capacity of the

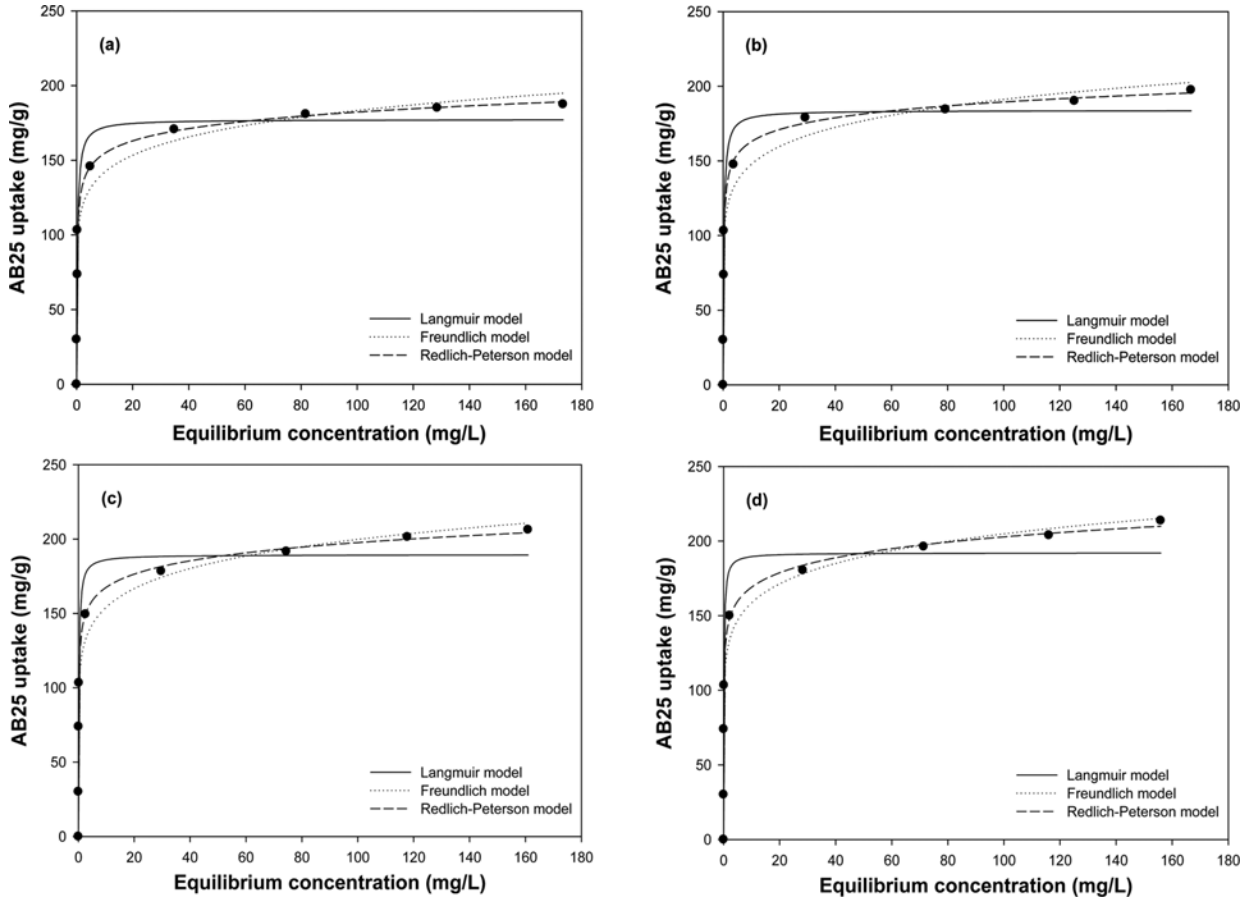

Fig. 7. Adsorption isotherms of AB25 on PEI-chitin at (a) 298 K, (b) 308 K, (c) 318 K, and (d) 328 K. Curves were predicted using Langmuir (solid line), Freundlich (dotted line) and Redlich-Peterson (short dash line) models ($C_{i\ AB25}$: 0-300 mg/L, PEI-chitin dosage: 0.02 g, pH: 2.0, reaction time: 24 h at 25 °C).

Table 2. Isotherm parameters for AB25 at different temperatures

Isotherm models	Parameters	Temperature (K)			
		298	308	318	328
Langmuir	q_{max} (mg/g)	177.32	183.85	189.47	192.13
	b_L (L/mg)	3.276	3.639	5.379	7.472
	R^2	0.947	0.955	0.954	0.944
Freundlich	K_F (L/g)	109.95	113.93	118.99	122.80
	1/n	0.1110	0.1124	0.1125	0.1111
	R^2	0.955	0.957	0.966	0.971
Redlich-Peterson	K_{RP} (L/g)	1081.4	1107.7	1937.9	3487.9
	a_{RP} $(L/mg)^{\beta}$	8.021	7.697	13.420	24.519
	β	0.934	0.940	0.932	0.923
	R^2	0.964	0.972	0.980	0.981

adsorbent is calculated based on this relationship. Fig. 7 shows the isothermal adsorption curve of PEI-chitin with respect to the temperature (298, 308, 318, and 328 K) for initial AB25 concentrations ranging from 0 to 300 mg/L. As a result of the isotherm experiment, the maximum adsorption amount, which is difficult to calculate experimentally, was estimated by the Langmuir and Freundlich models with two parameters and Redlich-Peterson model with three parameters. The parameters of each model were calculated using nonlinear regression analysis. The results are listed in Table 2. The coefficient of determination R^2, which is calculated using the Langmuir, Freundlich and Redlich-Peterson models, is found to be 0.94 or higher, indicating a high reliability. Moreover, the R^2 value obtained using the Redlich-Peterson model is higher than that obtained using the Langmuir and Freundlich model at all of the experimental temperature conditions. When the β value is 1, the Redlich-Peterson model equation is according to the Langmuir model equation, and when the β value is 0, the Redlich-Peterson model equation is according to the Freundlich model equation. The β value of the Redlich-Peterson isotherm by PEI-chitin was found to be 0.92 or above close to 1 at all the temperatures tested, which means that it follows the Langmuir type of monolayer adsorption.

As listed in Table 2, the Freundlich constants (1/n) with respect to the adsorption temperature are approximately 0.11 and fall within the range of $0<1/n<1$. This implies that an effective adsorption manipulation is possible [23], and 1/n values closer to 1 (compared to 0) indicate higher adsorption strength [24]. The values of K_F, which is another Freundlich constant, are found to be 109.95, 113.93, 118.99, and 122.80 L/g at 298, 308, 318, and 328 K, respectively, implying a good adsorption capacity.

The q_{max} values calculated using the Langmuir model are 177.32, 183.85, 189.47, and 192.13 mg/g at 298, 308, 318, and 328 K, respectively, and the values of b_L, which is a Langmuir constant, are 3.276, 3.639, 5.379, and 7.472 L/mg. Clearly, the q_{max} and b_L values tend to increase with the increase in the temperature. However, with the increase in the temperature from 298 to 328 K, the maximum adsorption amount increases by only approximately 1.08 times, i.e., from 177.32 to 192.13 mg/g, indicating that the degree of change is not significant. In general, good adsorbents have a high maximum adsorption and a high affinity [25]. To evaluate the effectiveness of PEI-chitin as a biosorbent for AB25, various adsorbents reported in literature were compared with PEI-chitin. Table 3 lists the results. In terms of the maximum adsorption amount, PEI-chitin exhibits a higher maximum adsorption amount than hazelnut shell [26], base-treated *Shorea dasyphylla* sawdust [27], NaOH-treated *Ficus racemosa* [28], water lettuce [29], and *Azolla pinnata* [30], all of which exhibit a maximum adsorption amount lower than 100 mg/g; the maximum adsorption amount of biofilm [31] is 113.4 mg/g. The maximum sorption capacity of waste tea-activated carbon [32] is 203.34 mg/g, which is somewhat higher than that of PEI-chitin. However, its affinity is relatively low with a value of 0.422 L/mg. Hence, the biosorbent developed in this study is considered an excellent adsorbent for AB25.

4. Thermodynamic Properties

Thermodynamic parameters can be useful indicators for the spontaneity evaluation of the adsorption process and mechanism of the adsorption process. The Gibbs free energy change is related to the spontaneity of the adsorption process. If the value is negative, the process is considered spontaneous, and the greater the value, the more spontaneous is the process [33]. As listed in Table 4, with the increase in the temperature to 298, 308, 318, and 328 K, ΔG increases in the negative direction to −35.00, −36.44, −38.66, and −40.77 kJ/mol, respectively. The results exhibit that the spontaneity of the reaction, i.e., the adsorption of AB25 by PEI-chitin, increases with the increase in the temperature. In addition, the adsorption characteristics can be deduced based on the ΔG value. In general, if the ΔG value is in the range of −20 to 0 kJ/mol, the adsorption is considered physical, if the value is in the range of −80 to −20 kJ/mol, the adsorption is considered physisorption together with chemisorption, and if the value is in the range of −400~−80 kJ/mol,

Table 3. Comparison between different sorbents in terms of the maximum adsorption capacity for AB25

Sorbent	q_{max} (mg/g)	b_L (L/mg)	h (mg/g min)	Temperature (K)	Ref.
Hazelnut shell	60.2	0.043	7.53	293	[26]
Base-treated *Shorea dasyphylla* (BTSD) sawdust	24.39	0.430	2.65	300	[27]
NaOH-treated *Ficus racemosa* (NTFR)	60.2	0.134	2.38	323	[28]
Waste tea-activated carbon (WTAC)	203.34	0.422	4.35	303	[29]
Water lettuce (WL)	24.5	0.070	2.34	297	[30]
Azolla pinnata (AP)	50.5	0.027	0.82	297	[31]
Biofilm	113.4	1.23	47.30	303	[32]
PEI-chitin	177.32	3.276	8.60	297	This work

Table 4. Thermodynamic parameters for the adsorption of AB25 by PEI-chitin

ΔH (kJ/mol)	ΔS (J/K mol)	R^2	ΔG (kJ/mol)			
			298 K	308 K	318 K	328 K
23.15	194.45	0.946	−35.00	−36.44	−38.66	−40.77

the adsorption is considered as chemisorption [34,35]. Accordingly, the calculated ΔG value is in the range of −80 to −20 kJ/mol, indicating that the mechanisms of adsorption of dye onto PEI-chitin are physi- and chemisorption. The change in the enthalpy is also an indicator determining if the adsorption process is a physical or chemical sorption. A ΔH value lower than 20 kJ/mol indicates physical adsorption, whereas a ΔH value ranging from 80-200 kJ/mol indicates chemical adsorption [36]. The ΔH calculated in this study is 23.15 kJ/mol, confirming that the AB25 adsorption process using PEI-chitin is physi- and chemisorption. Finally, both the ΔH and ΔS values are positive, indicating that the adsorption reaction between PEI-chitin and AB25 is endothermic and that the entropy increases during this process [37].

5. Adsorption Kinetics and Modeling

Adsorption kinetics is one of the important factors that determine the efficiency of the entire adsorption process. Moreover, it provides theoretical information on the adsorption mechanism. Fig. 8 shows the results of the adsorption experiment with respect to time, wherein PEI-chitin is used to absorb AB25. The experiment was carried out at 25 °C for approximately 16 h for AB25 concentrations of 50 and 100 mg/L. As shown in Fig. 8, the adsorption is very rapid in the early stage, gradually progresses after a certain period of time, and reaches equilibrium after approximately 120 min (50 mg/L) and 500 min (100 mg/L). The amount of adsorption is 150.38 mg/g at 100 mg/L, which is approximately twice that at 50 mg/L. However, the time for adsorption equilibrium increases by approximately 4.2-times. Hence, the equilibrium time is found to depend on the initial concentration of the dye.

To understand the adsorption kinetics of the rate constants, the experimental data are described using pseudo-first-order and pseudo-second-order kinetic models. Table 5 lists the h and R^2 values calculated using the pseudo-first-order and pseudo-second-order kinetic models. The R^2 values calculated using the pseudo-first-order kinetic model are 0.951 and 0.874 for initial dye concentrations of 50 and 100 mg/L, respectively, lower than those obtained using the pseudo-second-order kinetic model (0.988 and 0.937). In addition, the q_2 values calculated using the pseudo-second-order kinetic model for all dye concentrations are more consistent with the experimentally obtained q_e values (74.48 and 150.38 mg/g) than the q_1 values. Therefore, it is better to represent the adsorption kinetic experimental data using the pseudo-second-order kinetic model for the adsorption of AB25 by PEI-chitin.

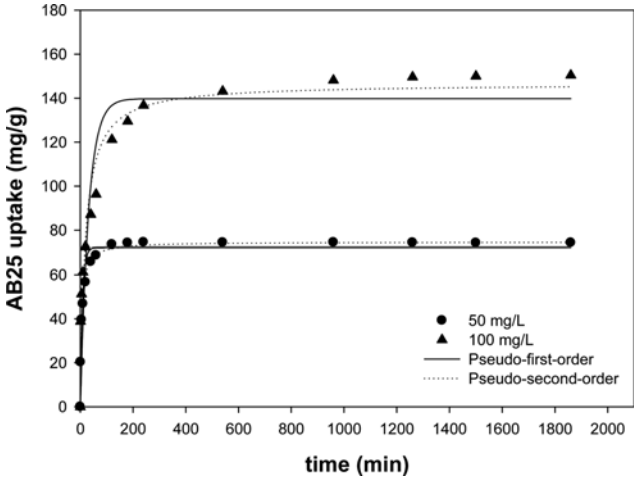

Fig. 8. Adsorption kinetics of AB25 on PEI-chitin for initial dye concentrations of 50 and 100 mg/L. Curves were predicted using pseudo-first-order (solid line) and pseudo-second-order (dotted line) models ($C_{i\,AB25}$: 100 mg/L, PEI-chitin dosage: 0.02 g, pH: 2.0, reaction time: 24 h at 25 °C).

In 50 mg/L of the initial dye concentration the rate constants k_1 and k_2 are 0.120 L/min and 0.0028 g/mg min, respectively. For an initial dye concentration of 100 mg/L, the rate constants k_1 and k_2 are 0.032 L/min and 0.0004 g/mg min, respectively. Clearly, the rate constants tend to decrease with the increase in the initial concentration of the dye. Moreover, with the increase in the initial concentration, the initial adsorption rate (h) decreases to 15.60 mg/g min at 50 mg/L and to 8.60 mg/g min at 100 mg/L. Nevertheless, these values are significantly higher than those of other adsorbents evaluated under similar conditions, as listed in Table 3.

6. Desorption and Reusability

To apply the developed adsorbent to an actual adsorption process, the adsorbent, which can be easily desorbed and is repeatedly usable, is employed. Desorption experiments were performed on PEI-chitin, which is used to adsorb AB25, to find a condition to effectively desorb the dye from the adsorbent. In this study, the desorption efficiency was assessed for NaOH, $NaHCO_3$, and Na_2CO_3 (candidate eluents for effective desorption) in the concentration range of 0.001-1 M (Fig. 9(a)). The eluents exhibit different highest desorption rates. The highest desorption rates of NaOH and $NaHCO_3$ are 85.2 and 78.7% at a concentration of 0.01 M, respectively, whereas the highest desorption rate of Na_2CO_3 at a concentration of 0.1 M is 47.6%. Overall, the desorption rate is highest when 0.01 M NaOH is employed as the eluent.

Table 5. Parameters of kinetic models for AB25 adsorption

Initial dye concentration (mg/L)	Pseudo-first-order				Pseudo-second-order			
	q_{exp} (mg/g)	q_1 (mg/g)	k_1 (L/min)	R^2	q_2 (mg/g)	k_2 (g/mg min)	h (mg/g min)	R^2
50	74.48	72.30	0.120	0.951	74.63	0.0028	15.60	0.988
100	150.38	139.77	0.032	0.874	146.60	0.0004	8.60	0.937

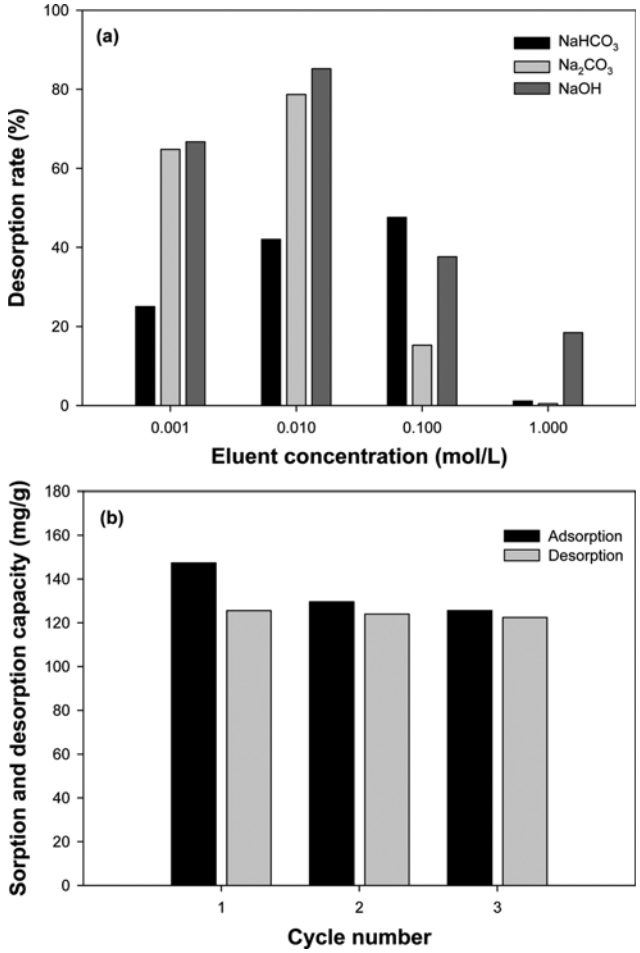

Fig. 9. (a) Desorption efficiency of different eluents with respect to eluent concentrations ($C_{i\ eluents}$: 0.001-1 M, reaction time: 24 h at 25 °C); and (b) reusability of PEI-chitin ($C_{i\ AB25}$: 100 mg/L, PEI-chitin dosage: 0.02 g, pH: 2.0±0.3, reaction time: 24 h at 25 °C).

To investigate the reusability of the developed chitin-based adsorbent, the adsorption-desorption experiments were repeated three times. Fig. 9(b) shows the results. In the first experiment, the adsorption and desorption amounts are found to be 147.4 and 125.5 mg/g, respectively, and the desorption efficiency is 85.2%, which is similar to that shown in Fig. 9(a). However, the experimental results of the second experiment are interesting. In the second experiment, the adsorption amount is 129.6 mg/g, which is approximately 12% lower than that in the first experiment, whereas the desorption amount is 124.0 mg/g, corresponding to a high desorption efficiency of 95.7%. The results of the third experiment are similar to those of the second. Although some adsorption loss is observed because of the repeated use of the adsorbent, this result still helps verify the high reusability of the PEI-chitin biosorbent for adsorption of AB25.

CONCLUSIONS

The PEI-chitin developed in this study is a biosorbent that can effectively help remove anionic dyes. The adsorption performance of PEI-chitin was evaluated using AB25, which is an acid dye. The FE-SEM images, FTIR spectra, and simple adsorption experiments of raw chitin, GA-chitin, and PEI-chitin confirmed the successful preparation of PEI-chitin. The adsorption of AB25 by PEI-chitin was found to strongly depend on the pH, and an excellent adsorption performance was observed at low pH values. The results of the isothermal adsorption experiments with respect to the temperature were better described using the Freundlich model than the Langmuir model, and the maximum adsorption amount calculated using the Langmuir model at a pH of 2 and 298 K was 177.32 mg/g. The changes in ΔG, ΔH, and ΔS (thermodynamic variables) revealed that the adsorption process between PEI-chitin and AB25 can be characterized by the following thermodynamic processes: physisorption and chemisorption, endothermic reaction, and increased entropy. In addition, the lower the dye concentration, the faster the adsorption equilibrium is attained, and the results of the adsorption kinetic experiments were well reproduced using the pseudo-second-order kinetic model. In the desorption experiment, the desorption rate was found to be highest (85%) when 0.01 M NaOH was used as the eluent, and the adsorption-desorption experiments, which were repeated three times, confirmed the reusability of PEI-chitin. In conclusion, the PEI-chitin-based adsorbent developed in this study can be used to effectively remove anionic dyes and has a high potential to be used as a renewable biosorbent.

ACKNOWLEDGEMENTS

This research was a part of the project titled 'Yeongnam Sea Grant', funded by the Ministry of Oceans and Fisheries, Korea and was supported by Basic Science Research Program through the National Research Foundation of Korea (NRF) funded by the Ministry of Science, ICT & Future Planning (NRF-2017R1A1A1A05000741).

REFERENCE

1. M. B. Gholivand, Y. Yamini, M. Dayeni and S. Seidi, *Environ. Prog. Sustain. Energy*, **34**, 1683 (2015).
2. M. Sadeghi-Kiakhani, M. Arami and K. Gharanjig, *J. Appl. Polym. Sci.*, **127**, 2607 (2013).
3. V. K. Gupta and Suhas, *J. Environ. Manage.*, **90**, 2313 (2009).
4. K. Marungrueng and P. Pavasant, *J. Environ. Manage.*, **78**, 268 (2006).
5. A. Gottlieb, C. Shaw, A. Smith, A. Wheatley and S. Forsythe, *J. Biotechnol.*, **101**, 49 (2003).
6. K. K. H. Choy, J. F. Porter and G. McKay, *Chem. Eng. J.*, **103**, 133 (2004).
7. A. S. Sartape, A. M. Mandhare, V. V. Jadhav, P. D. Raut, M. A. Anuse and S. S. Kolekar, *Arab. J. Chem.*, **10**, S3229 (2017).
8. Z. Aksu, *Process Biochem.*, **40**, 997 (2005).
9. S. Rangabhashiyam, N. Anu, M. S. Giri Nandagopal and N. Selvaraju, *J. Environ. Chem. Eng.*, **2**, 398 (2014).
10. N. M. Mahmoodi, U. Sadeghi, A. Maleki, B. Hayati and F. Najafi, *J. Ind. Eng. Chem.*, **20**, 2745 (2014).
11. M. Vakili, M. Rafatullah, B. Salamatinia, A. Z. Abdullah, M. H. Ibrahim, K. B. Tan, Z. Gholami and P. Amouzgar, *Carbohydr. Polym.*, **113**, 115 (2014).
12. G. L. Dotto, J. M. N. Santos, I. L. Rodrigues, R. Rosa, F. A. Pavan and

E. C. Lima, *J. Colloid Interface Sci.*, **446**, 133 (2015).
13. Y. Guo, B. Duan, L. Cui and P. Zhu, *Cellulose*, **22**, 2035 (2015).
14. Y.-L. Cao, Z.-H. Pan, Q.-X. Shi and J.-Y. Yu, *Int. J. Biol. Macromol.*, **114**, 392 (2018).
15. L. You, C. Huang, F. Lu, A. Wang, X. Liu and Q. Zhang, *Int. J. Biol. Macromol.*, **107**, 1620 (2018).
16. Y. Ma, W.-J. Liu, N. Zhang, Y.-S. Li, H. Jiang and G.-P. Sheng, *Bioresour. Technol.*, **169**, 403 (2014).
17. S. W. Won, I. S. Kwak and Y.-S. Yun, *Bioresour. Technol.*, **160**, 93 (2014).
18. R. Li, Q.-D. An, Z.-Y. Xiao, B. Zhai, S.-R. Zhai and Z. Shi, *RSC Adv.*, **7**, 40227 (2017).
19. Q. Yang, F. Dou, B. Liang and Q. Shen, *Carbohydr. Polym.*, **59**, 205 (2005).
20. H. A. Choi, H. N. Park and S. W. Won, *J. Environ. Manage.*, **204**, 200 (2017).
21. Y. C. Wong, Y. S. Szeto, W. H. Cheung and G. McKay, *Langmuir*, **19**, 7888 (2003).
22. X.-F. Sun, S.-G. Wang, W. Cheng, M. Fan, B.-H. Tian, B.-Y. Gao and X.-M. Li, *J. Hazard. Mater.*, **189**, 27 (2011).
23. I. A. W. Tan, A. L. Ahmad and B. H. Hameed, *J. Hazard. Mater.*, **154**, 337 (2008).
24. K. Fytianos, E. Voudrias and E. Kokkalis, *Chemosphere*, **40**, 3 (2000).
25. N. Barka, K. Ouzaouit, M. Abdennouri and M. El Makhfouk, *J. Taiwan Inst. Chem. Eng.*, **44**, 52 (2013).
26. F. Ferrero, *J. Hazard. Mater.*, **142**, 144 (2007).
27. M. A. K. M. Hanafiah, W. S. W. Ngah, S. H. Zolkafly, L. C. Teong and Z. A. A. Majid, *J. Environ. Sci.*, **24**, 261 (2012).
28. S. N. Jain and P. R. Gogate, *Int. J. Environ. Sci. Technol.*, **14**, 531 (2017).
29. M. Auta and B. H. Hameed, *Chem. Eng. J.*, **171**, 502 (2011).
30. M. R. R. Kooh, M. K. Dahri, L. B. L. Lim, L. H. Lim and C. M. Chan, *Appl. Water Sci.*, **8**, 61 (2018).
31. M. R. R. Kooh, M. K. Dahri, L. B. L. Lim and L. H. Lim, *Arab. J. Sci. Eng.*, **41**, 2453 (2016).
32. A. M. M. Mawad, N. M. H. Yousef and A. A. M. Shoreit, *Catrina Int. J. Environ. Sci.*, **10**, 53 (2015).
33. Y. S. Al-Degs, M. I. El-Barghouthi, A. H. El-Sheikh and G. M. Walker, *Dyes Pigm.*, **77**, 16 (2008).
34. Ö. Gerçel, A. Özcan, A. S. Özcan and H. F. Gerçel, *Appl. Surf. Sci.*, **253**, 4843 (2007).
35. M. Doğan, M. Alkan, Ö. Demirbaş, Y. Özdemir and C. Özmetin, *Chem. Eng. J.*, **124**, 89 (2006).
36. B. Gu, J. Schmitt, Z. Chen, L. Liang and J. F. McCarthy, *Environ. Sci. Technol.*, **28**, 38 (1994).
37. M. Ghaedi, H. Hossainian, M. Montazerozohori, A. Shokrollahi, F. Shojaipour, M. Soylak and M. K. Purkait, *Desalination*, **281**, 226 (2011).